metals

MDPI

Article

Comparison of Precipitates and Texture Evolution in Nb-Bearing Grain-Oriented Silicon Steel Produced by Conventional Processing and Novel Twin-Roll Casting

Yang Wang, Yuanxiang Zhang, Feng Fang, Xiang Lu, Guo Yuan * and Guodong Wang

State Key Laboratory of Rolling and Automation, Northeastern University, Shenyang 110819, China; wangyang@ral.neu.edu.cn (Y.W.); zhangyuanxiang@ral.neu.edu.cn (Y.Z.); fangfengdbdx@163.com (F.F.); luxiang@stumail.neu.edu.cn (X.L.); wangguodongral@163.com (G.W.)

* Correspondence: guoyuan_neu@hotmail.com

Received: 10 July 2020; Accepted: 8 August 2020; Published: 11 August 2020

Abstract: The Nb-bearing grain-oriented silicon steel sheets were produced by conventional route and novel twin-roll casting route, respectively. The microstructure, texture and precipitate evolution were comparatively investigated by using electron backscattered diffraction (EBSD) and transmission electron microscope (TEM). The findings revealed that the precipitation behavior and the texture evolution were totally different between the two processing routes. In the conventional route, a great number of nanoscale niobium nitride particles (NbN), which acted as mainly grain growth inhibitors were precipitated during hot rolling, while in the twin-roll casting route, due to the rapid solidification, the precipitation of NbN were suppressed and a new type Nb-bearing precipitate enriched with sulfur element was observed in the as-cast strip. Besides, the primary recrystallized texture of conventional specimens was characterized by strong γ-fiber with a peak at {111} <110>, together with very few Goss components. While in the case of twin-roll casting specimens, the strongest primary recrystallized texture was {111} <112> texture and the area fraction of Goss component was much higher than that of conventional specimens. After final high temperature annealing, complete secondary recrystallization was obtained in twin-roll casting specimens and the magnetic induction of B_8 was 0.1 T higher than that of conventional specimens.

Keywords: niobium precipitates; grain-oriented silicon steel; twin-roll strip casting; texture; microstructure

1. Introduction

Grain oriented silicon steel is widely used as the core material in electrical transformers because of its high magnetic induction and low iron loss [1]. The excellent magnetic properties are attributed to the sharp Goss texture obtained by secondary recrystallization [2]. The fine and dispersed second phase particles, which called as grain growth inhibitors in grain-oriented silicon steels, play a significant role in controlling the matrix grain size and promoting the abnormal growth of Goss texture [3]. In industrial, according to the inhibitor acquisition approaches, the production technology of grain-oriented silicon steel can be classified into two categories, the inherent inhibitor method and the acquired inhibitor method [4]. The inherent inhibitor method is adding inhibitors elements to melt steel directly, and the effectively inhibitors are precipitated during hot rolling or hot strip annealing. The main challenge of this method is that the slab must be reheated up to a very high temperature (1350–1400 °C, MnS and AlN as mainly inhibitors; 1250–1300 °C, Cu2S as mainly inhibitors) to dissolve the coarse particles formed during conventional continues casting [5]. This high temperature slab reheating led to many problems, such as high energy consumption, high gas emissions and low yield etc. In order to overcome these shortcomings, the acquired inhibitor method is proposed [6]. This method is avoiding the inhibitors formation in the hot rolled steps, and thus the slab reheating temperature can be decreased to 1150–1200 °C. The mainly inhibitor AlN is formed by nitrogen in the decarburization annealing process [6]. However, the nitriding process is particularly complicated and difficult to control accurately although this method has gradually become the mainly manufacturing method of high magnetic induction grain-oriented silicon steel.

Recently, a novel twin-roll casting was proposed to manufacture grain-oriented silicon steel, which is also considered to be an ideal process compared to the conventional processing route [7,8]. On one hand, the twin-roll casting was a simplified processing, which can supply a thin strip directly from molten steel with the same thickness and width as that of conventional hot rolled strip, and a series of intermediate metallurgical processes such as continuous casting, slab reheating, and hot rolling processes can be eliminated, resulting in potentially significant economic and environmental benefits [9,10]. On the other hand, due to the advantage of its rapid solidification, the precipitates elements were supersaturated or precipitated finely during twin-roll casting, which also provides a possibility to solve the problem completely caused by the high temperature slab reheating of the inherent inhibitor method [11]. Dorin [12] and Malekjani [13] demonstrated that the nitrides and sulfides of high strength and low alloy steels and stainless steels were in solid solution or precipitated in nano-scaled during strip casting. Song [8] and Wang [14,15] reported that the effectively inhibitors (MnS and AlN) could be precipitated in a single hot rolling, hot strip annealing or recrystallization annealing after cold rolling. However, these previous researches are mainly focused on how to obtain more dispersed and fine precipitates. The detailed characteristics of precipitates are less studied. Furthermore, besides the precipitation behavior, the microstructure and texture evolution of twin-roll casting grain-oriented silicon steels are also significantly distinct from those in the conventional processing route, which have not been explored to the best of our understanding and also need a systematic study.

In the aspect of inherent inhibitor types, besides the common inhibitors (MnS, AlN and Cu_2S), the Nb-rich particles have been identified to be potential and effective inhibitors in grain-oriented silicon steel due to its desired particle size and number density. Hou [16] stated that the addition of Nb was helpful to obtain precipitates with a higher inhibition effect during hot rolling, leading to adoption the hot band annealing process. Hulka [17] used NbC as mainly inhibitors and observed that the addition of Nb was beneficial to obtain the desirable Goss texture, and the core loss of the silicon steel was lower than that of silicon steels using AlN or MnS as inhibitors. Fang [18] claimed that NbN is an effective additional inhibitor in strip casting grain-oriented silicon steel. Feng [19] studied the precipitation behavior and the texture evolution of grain-oriented silicon steel with different Nb contents and obtained relatively good magnetic properties in the conventional route. On the contrary, Lu [20] reported that the Nb tended to form stable carbides, which might remain in the final product even after decarburization annealing, and could deteriorate the final magnetic properties. Wang [21] reported that Nb (C, N) had an overwhelming number of density and grain pinning effects, as secondary recrystallization did not proceed in Nb-bearing grain-oriented silicon steel, and the overmuch {113} <110> texture prevented the growing of Goss texture. Therefore, it seems that there have been inconsistencies in the previous studies as mentioned above. It is worthwhile to clarify that the effect of Nb-precipitates on the microstructure and texture in grain-oriented silicon steel and answer the question that whether the Nb-precipitates can be used as mainly inhibitors in grain-oriented silicon steel.

In this work, the Nb element was introduced to grain-oriented silicon steel, and these steels were produced by conventional processing route and twin-roll casting processing route, respectively. The microstructure, texture and precipitate were studied comparatively. The aim of this study was to clarifying the effect of Nb addition on the microstructure, texture, and precipitation of grain-oriented silicon steel, especially the different effect of Nb addition between the conventional processing route and twin-roll casting processing route.

2. Experimental Procedures

The ~2.0 mm thick grain-oriented silicon steel strips with similar chemical compositions were fabricated by a conventional hot rolled process and a twin-roll casting process respectively. And the detail compositions were listed in Table 1. Here, 0.06 wt% Nb content was selected based on the other research results [19]. The carbon content was reduced to 0.005 wt% to avoid the formation of NbC according to our previous workes [18]. Figure 1 shows the schedule diagram of conventional hot rolled process and twin-roll casting process. In the conventional process, the experimental grain-oriented silicon steel was melted in a 50 kg vacuum induction and the ingots were forged into a rectangular slab with the size of 60 mm in thickness and 80 mm in width. Next, the slab was reheated at 1250 °C, and the finishing hot rolling temperature was ~950 °C. The thickness of the final hot rolled strip was ~2.0 mm. In contrast, twin-roll casting can provide a thin steel strip directly from liquid steel, and the conventional steps such as slab reheating, rough rolling and finish rolling can be omitted. This compact and energy-efficient technology is the current state-of-the-art in the field of continuous casting. And the detailed processing parameters of the conventional processing and twin-roll casting were reported as previous literature [15,21]. The casting superheating temperature was ~20 °C, and after sub-rapid solidification, the as-cast strip was quenched to room temperature. And the thickness of the as-cast strip was 2.0 mm.

Table 1. Chemical composition of experimental steels.

Process & Elements	C	Si	Mn	Al	S	N	Nb
Twin roll casting process	0.005	3.05	0.08	0.013	0.021	0.008	0.061
Conventional process	0.005	3.18	0.085	0.010	0.020	0.005	0.060

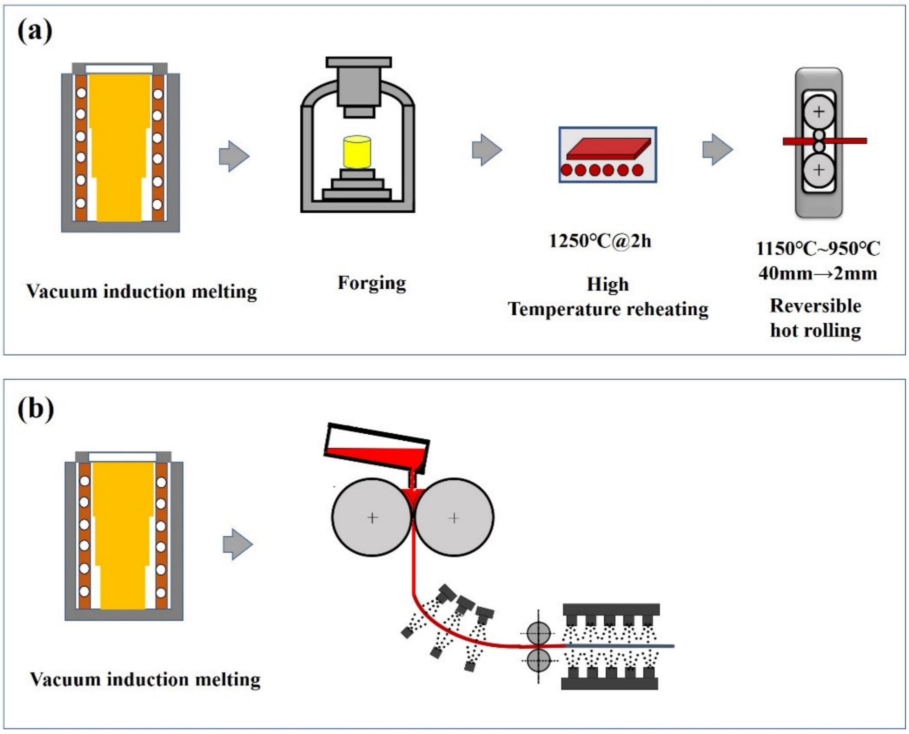

Figure 1. The schematic diagram of conventional hot rolling process (**a**) and twin-roll casting process (**b**).

Subsequently, both the hot rolled and as-cast strips were cold rolled to 0.23 mm using a two-stage cold rolled method with intermediated annealing. As shown in Figure 2. The hot rolled and as-cast strips were firstly cold rolled to 0.65 mm and then annealed at 1050 °C for 5 min in N_2 atmosphere, following by secondly cold rolled to 0.23 mm. After that, the final cold rolled sheets were primary annealed at 850 °C for 5 min and air cooling to room temperature. Finally, the primary annealed sheets coated using MgO were heated up to 1180 °C at a slow rate of 15 °C/h for secondary recrystallization.

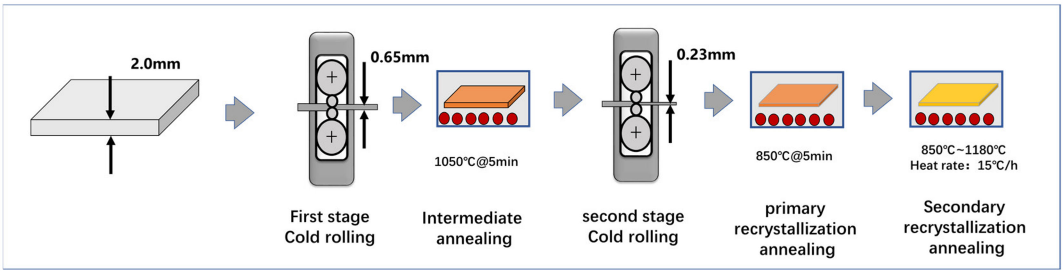

Figure 2. The schematic diagram of two-stage cold rolling method.

The microstructure and texture of the as-cast strip, hot rolled strip and primary annealing sheets along the longitudinal section defined by rolling direction (RD) and normal direction (ND) were characterized by electron backscattered diffraction (EBSD, Oxford, Aztec, UK) attached to a scanning electron microscopes(SEM, Zeiss, Ultra 55, Germany). The precipitation observation was carried out in a Tecnai G2 F20 transmission electron microscope (TEM, FEI, Hillsboro, OR, USA). The chemical composition of precipitates was analyzed using energy dispersive X-ray spectroscopy (EDX) and EDX scanning transmission electron microscopy (STEM) attached to a Tecnai G2 F20 TEM. The magnetic induction at 800 A/m (B_8) and iron loss at 1.7 T, 50 Hz were measured using a single sheet tester in the rolling direction of the secondary annealed specimens of 100 mm length and 30 mm width.

3. Results and Discussions

3.1. The Conventional Hot Rolled Strip and Twin-Roll As-Cast Strip

The microstructure and texture of a twin-roll as-cast strip were totally different from that of conventional hot rolled strip (shown in Figure 3a,d). The conventional hot rolled strip had a significantly microstructure and texture gradient, which can be divided into three layers. The surface layer was consisted of fine equiaxed grains with an average size of 30 μm and showed the random texture. The subsurface layer was composed of relatively coarse recovery grains with {110}//ND texture (green), and the center layer was characterized by number of elongated deformed grains with {100}//ND (red) and {111}//ND (blue) texture. Compared to the conventional hot rolled sheets, the as-cast strip was much coarser, and the grain size was in the range of 50–500 μm. The surface and subsurface layers were composed of columnar grains and coarse equiaxed grains. The subsurface layer grains inclined ~20° from ND of the strip, showing an obvious deformation characteristic (indicated by red dashed arrow). The "solidified meshing line" composed of fine equiaxed grains can be observed in the center layer. In addition, the as-cast strip revealed a very weak and random texture around the whole thickness area compared to the conventional hot rolled strip (shown in Figure 3c,f). This result indicated that the selective growth of {100} <uvw> fiber was hindered and the heterogeneous nucleation mechanism played a dominated role during the rapid solidification.

Usually, the Goss texture distributed in the subsurface layer of hot rolled strip was considered to be the crystal nucleus of secondary recrystallization. Its volume fraction and orientation deviation were closely related to the behavior of secondary recrystallization and the final magnetic properties [22]. In this work, the volume friction of Goss texture in conventional hot rolled strip was ~6.82%, while in the twin-roll casting processing, the hot rolled step was omitted and the volume fraction of Goss texture in as-cast strip was ~1.56%, which was much lower than that of the conventional hot rolled strip (shown in Figure 3b,e).

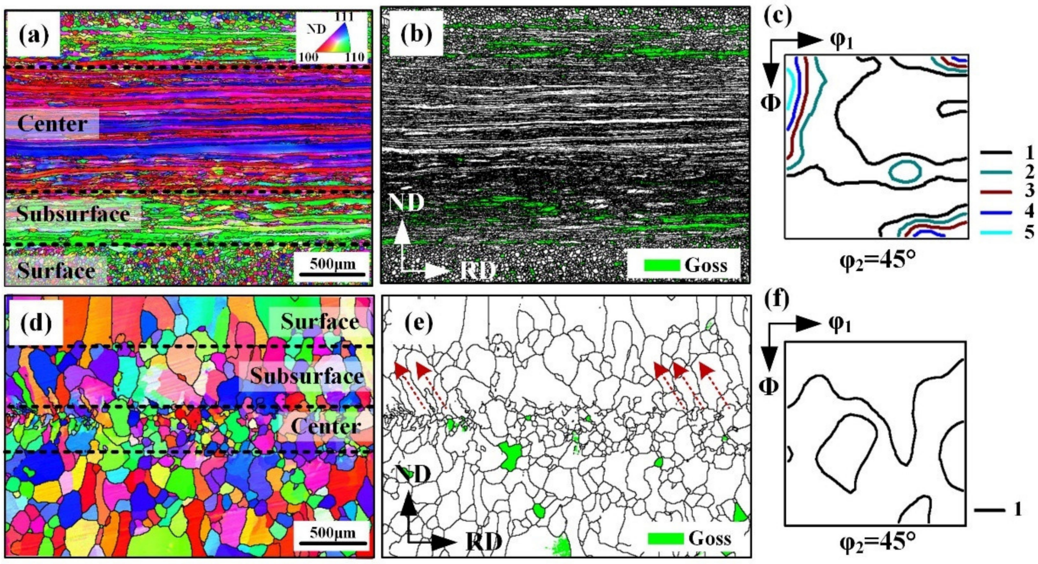

Figure 3. EBSD Orientation image maps (**a**,**d**) and Goss texture with the deviation of 15° (**b**,**e**), as well as φ_2 = 45° sections of ODFs (**c**,**f**) in the hot rolled (**a**–**c**) and as-cast strips (**d**–**f**).

The precipitates distribution of conventional hot rolled and as-cast strips were shown in Figures 4 and 5. Many nano-sized precipitates were observed in conventional hot rolled strip (Figure 4a). The average precipitates size was 8.6 nm, and the number density was 130/μm^2. The energy dispersive X-ray analysis (EDX) showed that the spherical particles were containing Nb element. And the selected area diffraction pattern (SADP) indicated that the precipitates were face-centered cubic structures and the lattice constant was 0.424 nm, and combined with the EDS and SADP analysis, it can be confirmed that the precipitate was NbN. However, compared to conventional hot rolled strip, the precipitates of as-cast strip were much lower in number and mainly nucleated at grain boundaries (Figure 5a). The precipitates particles were fine rod type and grow up to a certain extent. The typical size was ~5 nm in diameter and several dozen nanometers in length for these elongated precipitates. The HR-TEM (high-resolution transmission electron microscope) and corresponding FFT (fast Fourier transform) diffractogram (Figure 5b,c) showed that the precipitates were also face-centered cubic structures and the lattice constant was ~0.446 nm, which was slightly larger than NbN precipitate. The EDX and STEM-EDX showed that the precipitates were mainly contained Nb and S elements (Figure 5d,e).

These results indicated that the composition and morphology of Nb-bearing precipitates are significant differences between conventional and twin-roll casting processing route. The spherical NbN particles are the main precipitates in the conventional hot rolled strip, while in the as-cast strip, the Nb-bearing precipitate shows a short rod shape and contains certain S element. Wang et al. [23] calculated the formation enthalpy of NbS with face-centered cubic structures by the first-principles method and reported that the formation enthalpy of NbS is slightly less than that of NbC and NbN. This result indicates that the NbS may be formed in steel from a thermodynamic point of view. In addition, due to the diffusion ability of C and N atoms is much higher than that of the S atom, the Nb-bearing precipitates are mainly NbC, NbN, and Nb(CN), and the NbS is rarely observed in the conventional near-equilibrium solidification conditions. In this study, the twin-roll casting with extreme non-equilibrium solidification conditions was applied, which can provide a higher undercooling degree, and it is possible to form NbS with relatively lower enthalpy. Furthermore, the Nb and S elements are easy to segregate at grain boundaries and form locally enriched regions, which may also promote the formation of NbS precipitates. Taking into account the above factors, we can deem that it is reasonable to form the NbS precipitates during the strip casting processing routes.

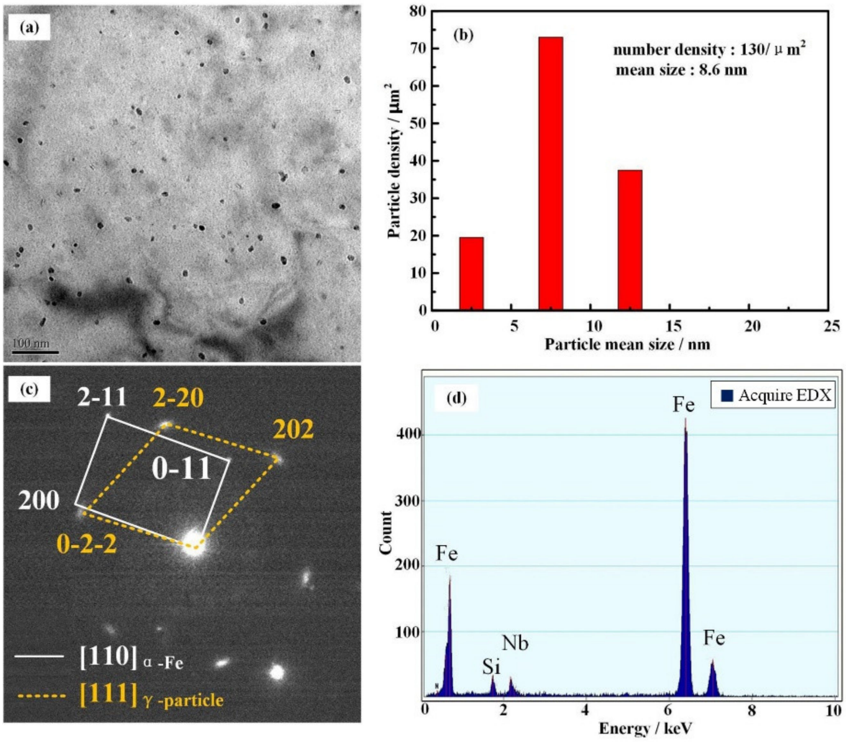

Figure 4. TEM micrograph for the precipitates (**a**) and its size distribution (**b**) in the hot rolled strip, as well as the SADP (**c**) and EDX spectrum (**d**) of precipitates.

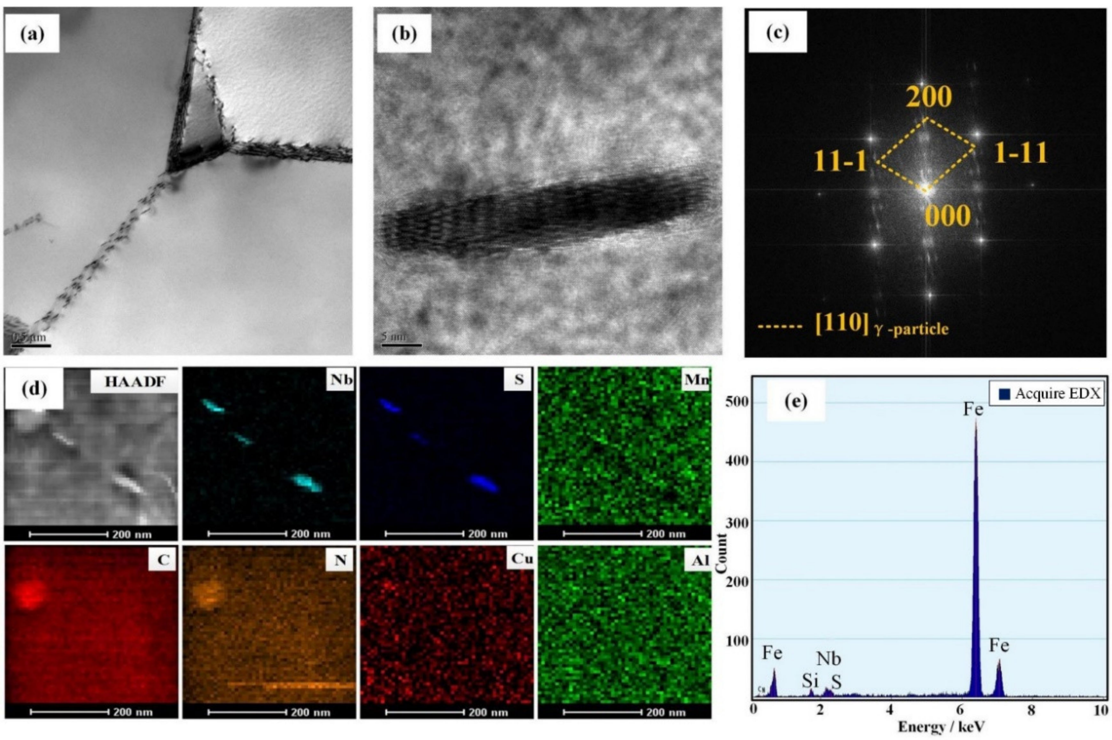

Figure 5. TEM micrograph (**a**), HR-TEM micrograph (**b**), FFT diffractogram (**c**), EDX-STEM maps (**d**) and EDX spectrum (**e**) of precipitates in as-cast strip.

3.2. The Primary Annealed Sheets

Figure 6 displayed the orientation image maps of primary annealed sheets produced by conventional and twin-roll casting routes. The conventional primary annealed sheets were characterized by a strong γ-fiber with a peak at {111} <110> texture. The novel primary annealed sheets produced by twin roll casting also showed a strong γ-fiber while the peak was located at {111} <112> texture (shown in Figure 6b,e). The fraction of primary Goss texture produced by conventional processing and twin-roll casting was 0.84% and 1.24%, respectively (shown in Figure 6c,f). It should be noted that the twin-roll casting silicon steel, which had a lower initial Goss texture in the as-cast strip, while had a higher Goss texture fraction in primary annealed sheet compared to that of the conventional processing route. On the other hand, the average grain size of primary annealed sheet produced by the conventional processing routes and twin-roll casting was 9.3 µm and 14.7 µm, respectively (shown in Figure 6a,d). The smaller primary recrystallized grain size in conventional route indicated that the pinning strength of Nb-precipitates was higher than that of twin-roll casting processing route.

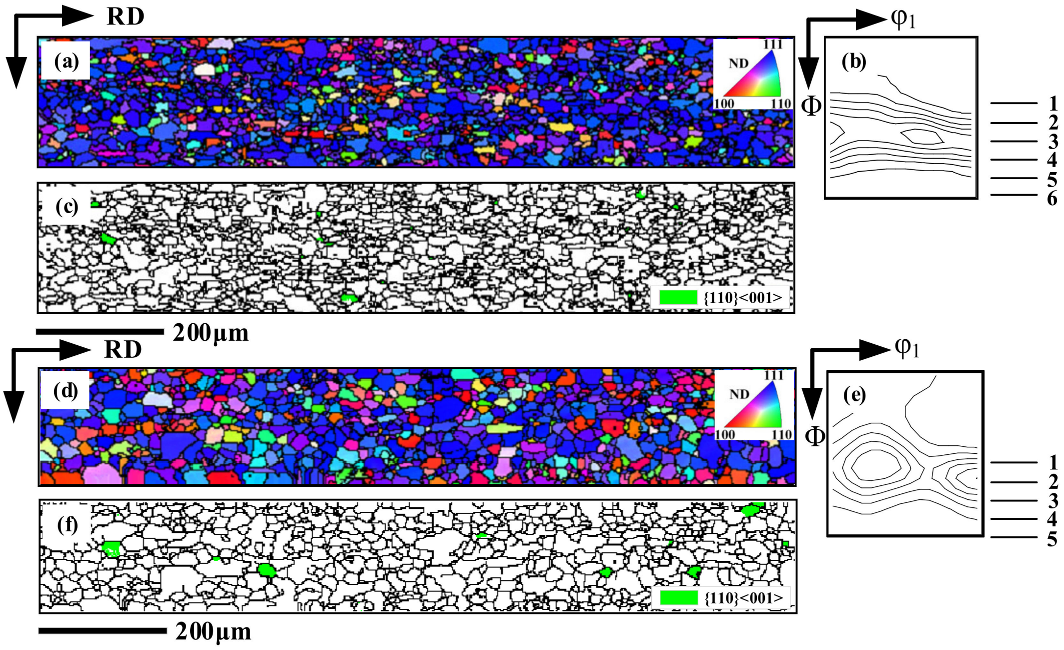

Figure 6. EBSD orientation image maps of primary annealing sheets (**a**,**d**) and Goss texture with the deviation of 15° (**c**,**f**), as well as corresponding φ_2 = 45° ODF sections (**b**,**e**) of conventional (**a**–**c**) and twin-roll casting (**d**–**f**) route.

From Figures 3 and 6, it can be seen that the fraction of Goss texture in the as-cast strip is much lower than that in the conventional hot rolled strip, but after the cold rolling and primary annealing, the Goss texture in the twin-roll casting route is stronger than that in the conventional route. These results show that the origin of Goss texture in twin-roll casting is quite different from that in the conventional route. In conventional route, Goss texture mainly originates from the subsurface layer of the hot rolled sheet. During hot rolling, the hot rolled sheet is subjected to shear deformation due to the friction between the roller and hot rolled sheet. The {100} <001>~<110> grains formed during solidification are rotated to Goss orientation around RD or TD, and eventually become the dominant texture of the subsurface layer [22]. This hot rolled Goss texture continues to rotate to γ-fiber by the plane deformation during cold rolling, while a certain Goss-oriented sub-structure is survived in the micro-bands between cold rolling deformation bands. After primary annealing, the Goss-oriented sub-structure preferentially nucleates and grows, which is called the "genetic effect of Goss texture" [22]. As for the twin-roll casting processing route, the as-cast strips show a very weak texture. It is difficult to provide strong Goss texture by rapid solidification and high temperature micro-plastic deformation. Furthermore, the hot rolling steps have been omitted, and the Goss texture cannot be obtained by using hot-rolled crystal rotation as the conventional route. In fact, the Goss texture can be also obtained by cold rolling and subsequent recrystallized annealing. Park [24] reported that the shear bands formed by cold rolling were suitable sites for the nucleation of Goss texture. However, the conventional hot rolled grain size before cold rolling is relatively small. It is difficult to develop the shear bands and then the number of Goss crystal nuclei formed by cold rolling is much smaller than that by hot rolling [25]. In the twin-roll casting processing route, the initial microstructure of the as-cast strip is relatively coarse, which is more favorable for the formation of the shear band during cold rolling and more Goss texture can be formed in the subsequent primary annealed process.

Figure 7 showed the micrographs and statistical results of precipitates in the primary annealed sheets. In every specimen, the precipitates were counted in ten random TEM images (magnified 5000 times, selected area was ~200 μm^2). It can be seen that both the primary annealed sheets contained a number of fine and dispersed precipitates. The particle density in primary annealed sheets produced by conventional and twin-roll casting route was 9.8/μm^2 and 3.6/μm^2 respectively, and the corresponding mean diameter of particles was 35.8 nm and 41.3 nm. The size and distribution of precipitates were in good agreement with the grain size of primary recrystallized sheets.

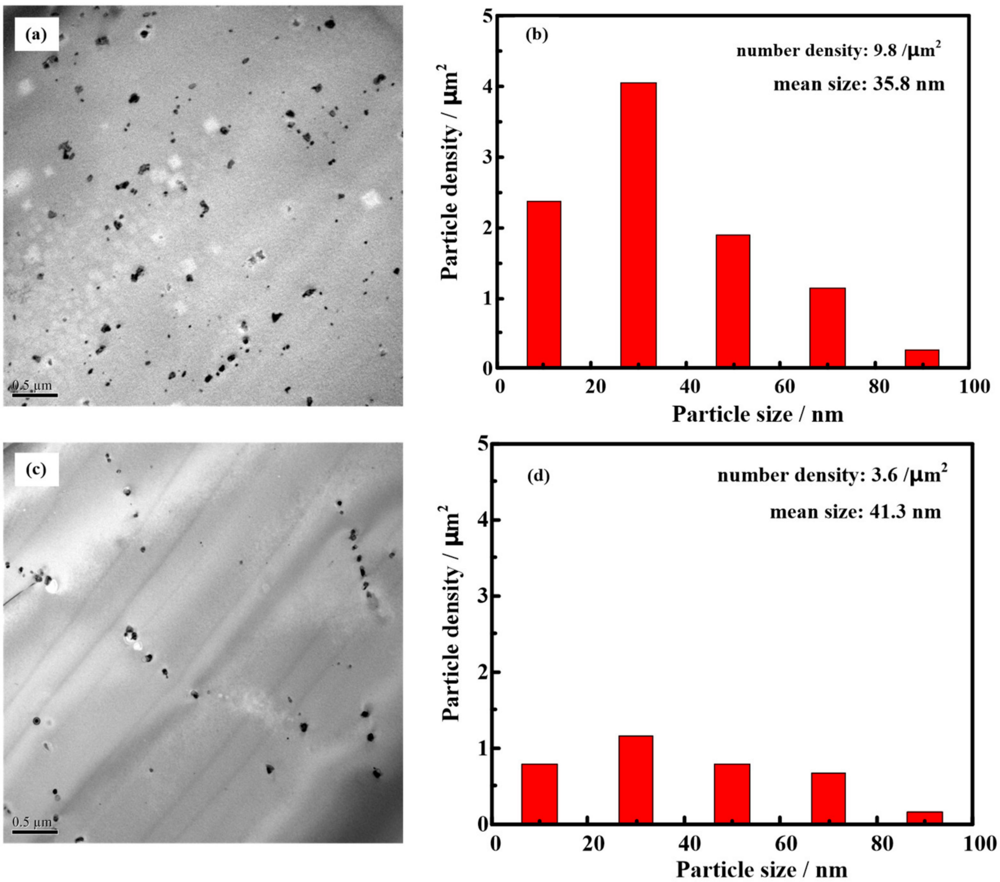

Figure 7. TEM micrographs (**a**,**c**) and statistical results (**b**,**d**) of precipitates in the primary annealed sheets produced by conventional (**a**,**b**) and twin-roll casting (**c**,**d**) route.

3.3. The Secondary Annealed Sheets

Figure 8 showed the macrostructure of secondary recrystallized sheets. In the conventional specimen, the secondary recrystallized grain size was in the range of 5–15 mm. The secondary recrystallization was incomplete and some of fine grains with the size of less than 1 mm can be observed (shown in Figure 8a). The magnetic induction B_8 was 1.71 T and the core loss $P_{17/50}$ was 1.43 W/kg. In the case of twin-roll casting specimen, the secondary recrystallization was complete and the grain size was in the range of 20–50 mm (Figure 8b). The magnetic properties were significantly improved

(B_8 was 1.80 T and $P_{17/50}$ was 1.40 W/kg). This result indicates that twin-roll strip casting routes are more suitable for Nb-bearing grain-oriented silicon steel than conventional processing routes.

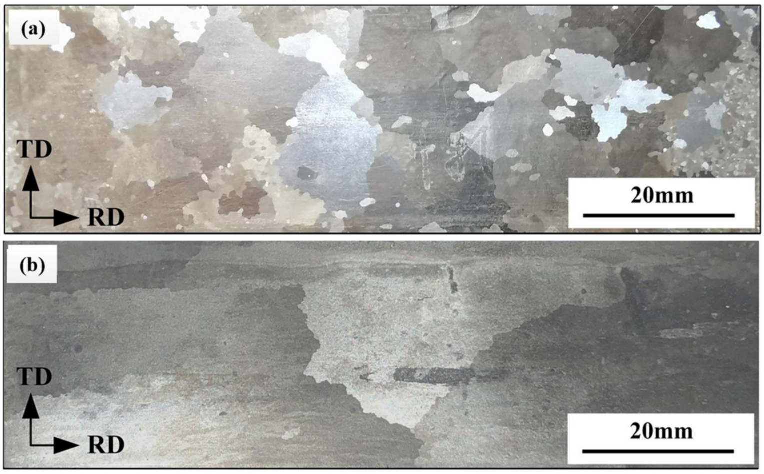

Figure 8. Macrostructure of secondary recrystallization sheets produced by (**a**) conventional and (**b**) twin-roll casting routes.

In twin-roll casting specimens, the strongest primary recrystallized texture is {111} <112>, while in conventional specimens, the strongest texture is {111} <110> (shown in Figure 6). It is well known that the Goss and {111} <112> present a Σ9 orientation relationship, and the special grain boundaries show a higher mobility compared to the common large angle boundaries [26]. Thus, the {111} <112> grains are easily consumed by Goss grains and further enhance the occurrence of secondary recrystallization during the high temperature annealing.

Eloot [27] found that the recrystallized {111} <110> texture is mainly originated from the deformed {111} <112> texture. and Ray [28] reported that the texture peak of deformed γ-fiber shift from texture {111} <112> to {111} <110> with the increasing of cold rolling reduction. That is to say, the {111} <112> is a sub-stable deformed texture, compared to the {111} <110> texture. In this study, the strongest {111} <110> recrystallized texture in conventional primary annealed sheets implied that the addition of Nb element may hinder the crystal rotation during cold rolling, leading to a relatively strong {111} <112> deformed texture. This result is consistence with our previous work [14]. In the case of twin roll casting processing routes, the initial microstructure of as-cast strip is much coarser than that of conventional hot rolled strip (shown in Figure 3). A large number of in-grain shear bands can be formed during cold rolling [29]. After primary annealing, the {111} <112> and Goss new grains are inclined to nucleated at in-grain shear bands [24]. As a result, the primary recrystallized {111} <112> texture of twin roll casting specimen is much stronger than that of conventional specimens.

4. Conclusions

1. The type of precipitates in conventional and twin-roll casting processing routes was different. In the conventional processing route, the mainly precipitates were NbN. However, in the twin-roll casting processing route, the precipitates of NbN were inhibited during the rapid solidification, and a new type precipitate of NbS was obtained.
2. In the twin-roll casting processing route, the Goss texture of grain-oriented silicon steel was formed during the cold rolling and primary annealing steps, which are totally different from that which originated from the hot rolling stage in the conventional processing route. Furthermore, the area fraction of primary recrystallized Goss texture in twin roll casting specimens was higher than that of conventional specimens.
3. The magnetic properties of twin-roll casting grain-oriented silicon steel were better than that of conventional grain-oriented silicon steel. The relatively good magnetic properties can be

attributed to the strong {111} <112> primary recrystallized texture in twin-roll casting specimens rather than {111} <110> texture in conventional specimens.

Author Contributions: Conceptualization, Y.W. and G.Y.; methodology, Y.Z.; software, F.F.; validation, Y.W. and X.L.; formal analysis, Y.W.; investigation, Y.W.; resources, G.Y.; data curation, Y.W.; writing-original draft preparation, Y.W.; writing-review and editing, Y.W.; visualization, X.L.; supervision, G.Y.; project administration, G.W.; funding acquisition, G.W. All authors have read and agreed to the published version of the manuscript.

Funding: This work was financially supported by the National Natural Science Foundation of China (5180102, 251974102), the Fundamental Research Funds for the Central Universities (N170703006) and the China Postdoctoral Science Foundation (2019M651129, 2019TQ0053).

Conflicts of Interest: The authors declare no conflict of interest.

References

1. Moses, A.J. Energy efficient electrical steels: Magnetic performance prediction and optimization. *Scr. Mater.* **2012**, *67*, 560–565. [CrossRef]
2. Park, H.-K.; Han, C.-H.; Park, C.-S.; Park, J.-T.; Joo, H.-D. Abnormal grain growth induced by grain boundary segregation of yttrium in grain-oriented Fe-3%Si steel. *Mater. Charact.* **2018**, *146*, 204–208. [CrossRef]
3. Matsuo, M. Texture control in the production of grain oriented silicon steels. *ISIJ Int.* **1989**, *29*, 809–827. [CrossRef]
4. Xia, Z.; Kang, Y.; Wang, Q. Developments in the production of grain-oriented electrical steel. *J. Magn. Magn. Mater.* **2008**, *320*, 3229–3233. [CrossRef]
5. Mishra, S.; Kumar, V. Co-precipitation of copper-manganese sulphide in Fe-3%Si steel. *Mater. Sci. Eng. B* **1995**, *32*, 177–184. [CrossRef]
6. Liao, C.-C.; Hou, C.-K. Effect of nitriding time on secondary recrystallization behaviors and magnetic properties of grain-oriented electrical steel. *J. Magn. Magn. Mater.* **2010**, *322*, 434–442. [CrossRef]
7. Wang, Y.; Xu, Y.; Zhang, Y.-X.; Fang, F.; Lu, X.; Liu, H.-T.; Wang, G.-D. Development of microstructure and texture in strip casting grain oriented silicon steel. *J. Magn. Magn. Mater.* **2015**, *379*, 161–166. [CrossRef]
8. Song, H.-Y.; Liu, H.-T.; Lu, H.-H.; An, L.-Z.; Zhang, B.-G.; Liu, W.-Q.; Cao, G.-M.; Cheng-Gang, L.; Liu, Z.-Y.; Wang, G. Fabrication of grain-oriented silicon steel by a novel way: Strip casting process. *Mater. Lett.* **2014**, *137*, 475–478. [CrossRef]
9. Park, J.Y.; Oh, K.H.; Ra, H.Y. Texture and deformation behavior through thickness direction in strip-cast 4.5wt%Si steel sheet. *ISIJ Int.* **2000**, *40*, 1210–1215. [CrossRef]
10. Park, J.Y.; Oh, K.H.; Ra, H.Y. The effects of superheating on texture and microstructure of Fe-4.5wt%Si steel strip by twin-roll strip casting. *ISIJ Int.* **2001**, *41*, 70–75. [CrossRef]
11. Lu, X.; Xu, Y.; Fang, F.; Zhang, Y.-X.; Wang, Y.; Jiao, H.; Cao, G.-M.; Li, C.-G.; Yuan, G.; Wang, G.-D. Microstructure, texture and precipitate of grain-oriented 4.5wt% Si steel by strip casting. *J. Magn. Magn. Mater.* **2016**, *404*, 230–237. [CrossRef]
12. Dorin, T.; Wood, K.; Taylor, A.; Hodgson, P.; Stanford, N. Quantitative examination of carbide and sulphide precipitates in chemically complex steels processed by direct strip casting. *Mater. Charact.* **2016**, *112*, 259–268. [CrossRef]
13. Malekjani, S.; Timokhina, I.B.; Wang, J.; Hodgson, P.D.; Stanford, N. Static recrystallization of strip cast alloys in the presence of complex nano-sulfide and nitride precipitates. *Mater. Sci. Eng. A* **2013**, *581*, 39–47. [CrossRef]
14. Wang, Y.; Xu, Y.; Zhang, Y.-X.; Fang, F.; Lu, X.; Misra, R.; Wang, G.-D. Effect of annealing after strip casting on texture development in grain oriented silicon steel produced by twin roll casting. *Mater. Charact.* **2015**, *107*, 79–84. [CrossRef]
15. Wang, Y.; Zhang, Y.-X.; Lu, X.; Fang, F.; Xu, Y.; Cao, G.-M.; Li, C.-G.; Misra, R.; Wang, G.-D. A novel ultra-low carbon grain oriented silicon steel produced by twin-roll strip casting. *J. Magn. Magn. Mater.* **2016**, *419*, 225–232. [CrossRef]
16. Hou, R.; Zhu, C.; Li, G.; Zhou, B.; Jia, J. Effect of Niobium on Precipitates and Texture Evolution of Fe-3% Si Grain-oriented Electrical Steel Annealed Hot Band. *ISIJ Int.* **2017**, *57*, 2245–2254. [CrossRef]

17. Hulka, K.; Vlad, C.; Doniga, A. The role of niobium as microalloying element in electrical sheet. *Steel Res.* **2002**, *73*, 453–460. [CrossRef]
18. Fang, F.; Lan, M.-F.; Lu, X.; Zhang, Y.X.; Wang, Y.; Yuan, G.; Cao, G.; Xu, Y.; Misra, R.; Wang, G. The impact of niobium on the microstructure, texture and magnetic properties of strip-cast grain oriented silicon steel. *J. Magn. Magn. Mater.* **2017**, *442*, 1–7. [CrossRef]
19. Feng, Y.-L.; Guo, J.; Li, J.; Ning, J. Effect of Nb on solution and precipitation of inhibitors in grain-oriented silicon steel. *J. Magn. Magn. Mater.* **2017**, *426*, 89–94. [CrossRef]
20. Lu, X.; Fang, F.; Zhang, Y.; Wang, Y.; Yuan, G.; Xu, Y.; Cao, G.; Misra, R.; Wang, G. Evolution of microstructure and texture in grain-oriented 6.5%Si steel processed by strip-casting. *Mater. Charact.* **2017**, *126*, 125–134. [CrossRef]
21. Wang, Y.; Fang, F.; Lu, X.; Zhang, Y.; Xu, Y.; Cao, G.; Li, C.; Misra, R.D.K.; Wang, G.-D. A Comparative Study of Microstructure and Texture Evolution in Cu-Bearing and Nb-Bearing Grain Oriented Silicon Steels. *Steel Res. Int.* **2016**, *88*, 1600181. [CrossRef]
22. Shimizu, Y.; Ito, Y.; Iida, Y. Formation of the Goss orientation near the surface of 3 pct silicon steel during hot rolling. *Met. Mater. Trans. A* **1986**, *17*, 1323–1334. [CrossRef]
23. Wang, P.; Liu, J.; Qi, Q.; Chang, X.; Gao, S.; Zhang, W.; Wang, P. Precipitate formations with self-adaptive elemental diffusion and segregation in T92 steel. *J. Alloy. Compd.* **2017**, *693*, 264–278. [CrossRef]
24. Park, J.-T.; Szpunar, J. Evolution of recrystallization texture in nonoriented electrical steels. *Acta Mater.* **2003**, *51*, 3037–3051. [CrossRef]
25. Park, N.-J.; Joo, H.-D.; Park, J.-T. Evolution of Goss Orientation during Thermal Heating with Different Heating Rate for Primary Recrystallization in Grain-oriented Electrical Steel. *ISIJ Int.* **2013**, *53*, 125–130. [CrossRef]
26. Homma, H.; Hutchinson, B. Orientation dependence of secondary recrystallisation in silicon–iron. *Acta Mater.* **2003**, *51*, 3795–3805. [CrossRef]
27. Eloot, K.; Okuda, K.; Sakata, K.; Obara, T. Texture evolution during cold rolling and recrystallisation of IF steel with a strong {111} hot band texture. *ISIJ Int.* **1998**, *38*, 602–609. [CrossRef]
28. Ray, R.K.; Jonas, J.J.; Hook, R.E. Cold rolling and annealing textures in low carbon and extra low carbon steels. *Metall. Rev.* **1994**, *39*, 129–172. [CrossRef]
29. Jonas, J. Effects of shear band formation on texture development in warm-rolled IF steels. *J. Mater. Process. Technol.* **2001**, *117*, 293–299. [CrossRef]